Fabrication of Long-range Ordered, Broccoli-like SERS Arrays and Application in Detecting Endocrine Disrupting Chemicals

Jing Chen[1,2], Gaowu Qin[1,],Wen Shen[2], Yiyan Li[3], Biswajit Das[2,*]*

1. Key Laboratory for Anisotropy and Texture of Materials (Ministry of Education), Northeastern University, Shenyang 110819, China

2. Nevada Nanotechnology Center, Howard R. Hughes College of Engineering, University of Nevada, Las Vegas, NV 89154-4026, USA

3. Department of Electrical and Computer Engineering, University of Nevada, Las Vegas, NV 89154, USA

Corresponding author

Tel.: +86 24 83691565 (G. W. Qin), 001 702 8952530 (B. Das).

*E-mail: qingw@smm.neu.edu.cn (G. W. Qin), dasb@unlv.nevada.edu (B. Das).

Abstract

Periodic broccoli-shaped Au, Ag surface-enhanced Raman spectroscopy (SERS) arrays were fabricated by combining ordered SiO_2 colloidal crystals templates with physical deposition technique. The SiO_2 colloidal crystal-assisted Au, Ag SERS substrates have a long-range, adjustable periodic structure and a clean surface without incorporating any reductants or surfactant chemicals. Different from depositing

directly on the flat substrates, the colloidal crystals-assisted nanostructure array has a larger effective surface area under the same projected area of the laser irradiation, which exposes more "hot spots". An increased roughness and a larger surface area have also been created as the highly bumpy surface feature from the broccoli-shaped SERS morphologies, resulting in a greater Raman amplification than the conventional metal film over nanosphere (MFON). SERS performances by Au and Ag SERS arrays reveal the long-range broccoli-like morphology is a promising SERS platform as it is highly sensitive, reproducible and stable. The colloidal crystal-assisted Ag SERS array has a slight higher enhancement factor (EF) than Au SERS array, while they are both at the order of 10^7 enhancement. Compared to our previous work which directly deposited noble metal nanoparticles onto flat substrates, the EF of the colloidal crystal-assisted SERS array is improved by one to two orders of magnitude. Finite-difference time-domain (FDTD) simulation was performed to estimate the electromagnetic field distribution. Finally, two endocrine disrupting chemicals (EDCs) (dioctyl phthalate (DOP) and dibutyl phthalate (DBP), homologous series) at different concentrations were successfully identified by Au, Ag SERS arrays with the detection limits of 0.24×10^{-9} M and 0.22×10^{-9} M, respectively. This study suggests the broccoli-like Au, Ag SERS array is a promising candidate for chemical sensing and this SERS substrates fabrication technique can be accessible to the standard industrial processes.

Keywords: SERS; broccoli-like; endocrine disrupting chemicals; long-range ordered; sensing

1. Introduction

Endocrine disrupting chemicals (EDCs) encompass a variety of substances, both natural and man-made, including dioxin, alkylphenols, DDT, phthalates, polychlorinated biphenyls, and so forth, can interfere with the hormone system in both humans and wildlife. EDCs may exist in many products people use daily, such as plastic bottles, metal food cans, detergents, food, toys, cosmetics, and pesticides.[1,2] Exposure to EDCs can increase risks to develop reproductive cancers, cause lowered fertility, birth malformations, and sexual development problems.[2,3] In May 2011, a major phthalate-contaminated foodstuffs incident happened in Taiwan. Di(2-ethylhexyl) phthalate (DEHP) and diisononyl phthalate (DiNP) were illegally added to foods and beverages as a substitute of emulsifier.[4,5] Phthalates are one of EDCs that are closely related to human life since they are used as plasticizers in polyvinyl chloride (PVC) plastics.[6] As phthalates are not chemically bound to PVC, their molecules can evaporate to the atmosphere, or move into the foodstuff.[7] Phthalate exposure has been found to be associated with numerous reproductive health and developmental problems,[6] and phthalates exhibit low acute toxicity with a lethal dose at 50 values of 1-30 g/kg bodyweight.[7]

The increasing incidents about the general population is continuously and ubiquitously exposed to the EDCs have raised public concerns about the environmental contaminants and public health.[8] Hence, a robust, reliable assessment is strongly required to identify EDCs, such as in the environmental media, foodstuff and consumer products.[9,10] The difficulties in detecting EDCs lie in the variety and

the low concentrations. The traditionally used detection methods include high performance liquid chromatography,[11] high performance liquid chromatography-tandem mass spectrometry,[5,8] gas chromatography-mass spectrometry,[12,13] and gas chromatography-electron capture detector. These methods are highly robust, however, some features such as requiring complex sample pretreatment, time-consuming and high cost limit their applications.[14]

Surface-enhanced Raman spectroscopy (SERS) is a handy, low cost, fast, nondestructive, ultra-sensitive and information-rich analytical technique which can fulfill trace detection or even single molecule detection.[15-23] Moreover, it provides fingerprint-like information which can offer distinguishable vibrational information used for molecule identification, and SERS peak intensity has the relationship with the analyte concentration. All of these features make SERS applicable to identify a wide variety of biological molecules,[24-40] for instance, proteins, DNA, RNA, microorganisms, and cancer cells, and also make SERS an ideal approach for the detection of chemical molecules,[41-47] such as toxic gases, explosives, drugs and EDCs. However, the detection of EDCs by SERS methodology is an emerging research field which needs more explorations. Besides, several recently published papers in this realm were associated with the chemical preparations of SERS substrates,[48,49] which would bring in the surface chemistry and interfere with SERS measurements. Therefore, a new type of SERS substrate with the reliability, reproducibility, stability, and high-sensitivity is urgently needed.

Until now, plenty of methods have been developed for preparation of

SERS-active substrates,[50-53] and the modeling of SERS substrates can be summarized as below. (1) Metallic nanoparticles and metallic films.[54-56] Christou *et al.* reported Au, Ag film SERS substrates were generated by using single UV-laser pulses treatment of thin Au and Ag films supported on quartz glass.[56] Although this type of SERS substrates is among the most widely used SERS substrates as their simple and cost-effective bottom-up fabrication approaches, it is hard to predict the location of "hot spots" as their random nanostructures, thus result in low reproducibility. (2) Multi-branched metallic nanocrystals. In order to increase the surface roughness and surface area of spherical nanoparticles to create more "hot spots" and to allow more analyte molecules to be attached, the multi-branched metallic nanocrystals with spiky surface features have been developed.[57-61] Xie and co-workers reported flower-like Au nanocrystals were chemically synthesized based on crystal growth in the limited ligand protection region.[58] Fang and co-workers demonstrated by using a nanoparticle-mediated aggregation protocol, "sea urchin"-like gold mesoparticles can be synthesized via a secondary nucleation and growth process.[60] In the preparation of multi-branched metallic nanocrystals, surfactants are necessary for regulating the growth and stability of nanocrystals. However, surfactants are hard to remove and will stay retained on the nanocrystal surface, thus will interfere with SERS detections. (3) Nanoparticles arrays. To reduce randomly aggregated colloids in SERS substrates, strategies like electrostatic assembly,[62] DNA hybridization-driven assembly,[63] or mechanical assembly such as convective flow upon solvent evaporation technique[64] have been investigated to

tailor the spacing and obtain ordered nanoparticles arrays. In Wang's work, by using

cetyltrimethylammonium bromide (CTAB) as the capping surfactant, highly ordered,

close-packed monolayer Au nanoparticle arrays with sub-10-nm gap were

successfully formed.[62] Recently, Lim and co-workers described by employing

DNA-modified technique, gold nanobridged nanogap particles with a uniform

nanobridge-supported 1 nm interior gap were produced.[63] The above strategies are

elaborate and can precisely control the interparticle distances and build well-defined

SERS arrays. However, the surface chemistry will still be involved as wet chemical

routes are needed. Moreover, the operation procedures are relatively complicated. (4)

Periodic SERS arrays. Periodic SERS array is one of the most prominent SERS

substrates, and have attracted great attentions in recent years. Electron beam

lithography (EBL) is famous for producing periodic SERS arrays. Yu *et al.*

demonstrated gold nanohole and nanodisk arrays with precisely controlled size and

spacing could be fabricated by EBL.[65] Theiss and co-workers developed an electron

beam lithography combined with an angle evaporation technique for the fabrication of

Ag nanoparticle dimer arrays with separations on the order of 1 nm.[66] Despite the

effectiveness of EBL, the time consuming, complex procedures, the significant cost,

low-throughput, and moderate enhancement factor (EF, $\sim 10^5$-10^6) hinder its wide

applications. An alternative way for producing periodic SERS arrays is

template-assisted fabrication, such as porous anodic aluminium oxide (AAO),[67]

natural nanostructures like butterfly wing,[68] polystyrene (PS),[69] or silica

nanospheres[70] are popularly used as templates. Also, the template-assisted strategy

allows for large-scale SERS arrays fabrication. In Rao's work, chemically reduced gold seeds were attached onto the ordered functionalized silica colloidal spheres by electrostatic interaction, then the growth of gold nanoshells was applied as a SERS analytical tool to assess H_2O_2 scavenging activity.[70] In the template-assisted approach, metal nanoparticles are often attached onto the templates by covalent linkage or electrostatic interaction, thus surface chemistry will be involved and will interfere with SERS measurements. Moreover, the SERS substrates made by nanosphere lithography (NSL) technique often have a large interparticle distance, which is not suitable for SERS enhancement.

Despite the significant progresses, obtaining reproducible, stable, reliable SERS substrates with novel geometries, periodic nanostructures, and high EFs over a large area in a convenient way still remains a challenge in SERS field. SERS nanostructure with a delicate morphology and a highly rough surface feature is an attractive SERS candidate, and normally the chemical approach is needed for fabricating this type of nanostructures as surfactants are necessary for regulating the transformations of shapes. But surfactants will inevitably attach on the SERS substrate surface and interfere with SERS detections. For physical deposition technique, it is difficult to get delicate morphology directly, and normally smooth metal films or unordered nanoparticle-aggregations will be fabricated.

In this paper, by combining three-dimensional (3D) ordered SiO_2 colloidal crystal template and physical deposition technique skillfully, delicate Au, Ag nanostructures with the unique broccoli-like morphologies have been successfully

fabricated respectively under a series of appropriate parameters. Moreover, these broccoli-like Au, Ag nanostructures present long-range, periodic SERS arrays, and have a clean, chemicals-free surface. Therefore, the reliability, reproducibility have been guaranteed, and the highly bumpy surface feature ensures the high-sensitivity. In general, the enhancement capability of the periodic patterned and highly reproducible SERS arrays is relatively low, whereas SERS substrates with a high enhancement capability are normally not reproducible[51]. Here, high reproducibility, periodic arrangement and large enhancement capability have been fulfilled at the same time in one SERS array. So the above mentioned limitations in SERS substrates fabrication process have been well addressed.

The improvements and advantages of this novel SERS arrays are also reflected in the following aspects. (1) Compared to the conventional metal film over nanosphere (MFON), [71] more "hot spots" will be created and more analyte molecules will be attached onto the broccoli-like SERS substrate, since the very bumpy SERS surface feature enables a greater surface roughness and a larger surface area. (2) Compared to the methods we developed previously by deposition of metal nanoparticles onto the flat substrates directly,[34, 72] the 3D long-range ordered SiO_2 colloidal crystal at here not only provides an arc surface to enable an larger surface area under the same projected area of the laser irradiation, but also makes an essential foundation for producing long-range periodic SERS arrays[73] and improves the reproducibility of SERS signals. What's more, by controlling the size of colloidal crystal spheres and the thickness of the metal nanoparticles deposited, the SERS substrates can be

reproducibly produced.[74] (3) The physical fabrication technique was used for producing SERS substrates, no reductants or surfactant chemicals were involved, thus making it easy for the analyte molecules, especially for the analyte with a weak affinity to the substrate surface to access the "hot spots" region by simple dripping or incubation of the substrate in the solution.[53] Additionally, as the clean surfaces without chemical interferences, the acquired SERS spectra are reliable. (4) This technique is convenient, cost-effective, allows high-throughput nanofabrication, and can be accessible to the standard industrial processes.

Next, the EFs, reproducibility, and long-term stability of these two SiO_2 colloidal crystal-assisted SERS arrays (Au and Ag) were evaluated. Finite-difference time-domain (FDTD) simulation was performed to estimate the electromagnetic field distribution. Then these two SERS arrays were successfully applied to identify two homologous series of EDCs, dioctyl phthalate (DOP) and dibutyl phthalate (DBP), and the detection limits were also calculated.

2. Experimental Section

2.1 Chemicals and Materials

DOP (99%), DBP ($\geq$99.5%), rhodamine 6G (R6G) ($\geq$ 95.0%, analytical standard), methanol (analytical standard) and ethanol (analytical standard) were purchased from Sigma-Aldrich. Ammonium hydroxide ($NH_3 \cdot H_2O$, 50% v/v aq. soln.), and hydrogen peroxide (H_2O_2, 35% w/w aq. soln.) were purchased from Alfa Aesar. Tetraethyl orthosilicate (TEOS, 98%), sulfuric acid (H_2SO_4, 95%-98%) were purchased from GFS Chemicals. Gold target (2.00" Dia. x 0.125" Thick, 99.99%) and silver target

(2.00" Dia. x 0.25" Thick, 99.99%) were purchased from Kurt J. Lesker Company (CA, USA). Silicon wafers were purchased from Silicon Valley Microelectronics (SVM, CA, USA). Ultrapure water (18.2 MΩ·cm) was used throughout the experiment.

2.2 Synthesis of Monodisperse SiO_2 Spheres

Monodisperse SiO_2 spheres were produced by using a slightly modified Stöber method.[75] Briefly, 4.5 mL of TEOS (98%) was rapidly added into a mixture of 9.0 mL of ammonium hydroxide solution (28%), 61.75 mL of ethanol, and 24.75 mL of H_2O. The reaction mixture was kept under stirring for 2 h at room temperature. The produced monodisperse SiO_2 spheres were washed three times with water and ethanol by centrifugation at 7000 g for 5 min, and then the samples were kept in ethanol for the following procedures.

2.3 Fabrication of SiO_2 colloidal crystal

Vertical deposition method was employed. Briefly, a silicon wafer cleaned in fresh Piranha solution (concentrated H_2SO_4 : 30% H_2O_2 = 3:1 volume ratio. *Caution: Piranha solution is extremely corrosive*) was vertically attached to the inside wall of a plastic vessel containing SiO_2 colloidal suspension (SiO_2-ethanol system, ~10 wt%). Then by using the isothermal heating evaporation method at 50 ^{o}C, SiO_2 colloidal crystals were self-assembled on the substrate surface. The whole system was kept in a stationary environment and isolated from external interference.

2.4 Preparation of Au and Ag SERS substrates

A versatile nanofabrication system (NanoSys 2, Oxford Applied Research Inc.), which

can deposit nanoparticles of any materials on any kinds of substrates, was applied to deposit Au and Ag nanoparticles onto the above SiO_2 colloidal crystals template. This system basically consists of three parts: (1) the nanocluster source, (2) the quadruple mass filter (QMF), and (3) the main deposition chamber. Nanoparticles with a large size distribution generated in the nanocluster source will be filtered through the QMF, which has been designed specifically for the high-resolution filtration of nanoparticles between 50 and 3×10^6 amu.[76] Here, in both Au and Ag nanoparticles deposition cases, the QMF was set at 10.0 nm size selection. The sputtering power was set at 115 W which is a moderate value for the system, and this power can be adjusted to generate appropriate sputtering rate after series of testing. The flow rate of one of the aggregation gases, Ar, was 100 standard-state cubic centimeters per minute (sccm), and the other aggregation gas, He, was 40 sccm. The deposition rate (4.5 Å/s) was measured by using a quartz crystal monitor (QCM, Sigma Instruments, SQM-160).

2.5 SERS Signal Reproducibility and Enhancement Capability Measurement

R6G was used as the probe molecules. 10 μL of 10^{-4} M R6G solution was dripped onto the above colloidal crystal-assisted Au and Ag SERS substrates, respectively. The SERS spectra were acquired immediately after the substrates were dried under ambient conditions. Normal Raman spectrum of 10^{-2} M R6G solution was also acquired.

2.6 SERS detection of two kinds of EDCs

The methanol solutions of DOP and DBP at different concentrations were prepared at first (10^{-10} ~ 10^{-3} M). For DOP detection, 200 μL of DOP methanol solutions at

different concentrations were dropped on the broccoli-like Au substrate, respectively.

SERS signals were recorded after solvent methanol completely evaporated. For DBP

detection, same procedures were performed but broccoli-like Ag substrate was used.

2.7 Long-term Stability Measurement of the SERS Substrates

The colloidal crystal-assisted Au and Ag SERS substrates were kept in commercial

aluminum foil for 90 days, and then their long-term stability were tested. R6G was

employed as the probe molecules. The commercial aluminum foil was rinsed with

acetone and ultrapure water in advance for degreasing.

2.8 Characterization

The morphologies of the SiO_2 colloidal crystal and SiO_2 colloidal crystal-assisted Au

and Ag SERS substrates were observed by JEOL 7500F field emission scanning

electron microscopy (FE-SEM). All SERS and bulk spectra were obtained using a

confocal Horiba Jobin Yvon LabRAM HR Raman spectrometer equipped with a 785

nm laser and a $100\times$ objective to focus the laser onto the sample surface and to collect

the scattered light from samples. The incident laser power was attenuated to 0.8 mW

for 10^{-4} M of R6G SERS detection, and the laser power for the normal Raman spectra

acquisition of 10^{-2} M bulk R6G solution was set as 80 mW. The frequency of the

Raman instrument was calibrated by referring to a silicon wafer at the vibrational

band of 520 cm^{-1}. All the measurements were carried out under ambient conditions.

3. Results and Discussion

3.1 Fabrication of SiO_2 colloidal crystal

The initial diameter of SiO_2 spheres is approximate 230 nm. Figure 1a reveals

the surface feature of the SiO_2 colloidal crystal. We observed that a relatively uniform colloidal crystal film was assembled by SiO_2 spheres self-arranged in a close-packed array, and the film also has a uniform thickness over large domains. However, the inevitable array defects still exist in certain microscopic areas in this SiO_2 colloidal crystals array. One possible reason could be the non-uniformity of SiO_2 spheres size distribution, and the other possible reason might be the SiO_2 spheres movement caused by the electron-beam scanning during the SEM images collection.[9] Figure 1b shows a crevice of SiO_2 colloidal crystals, which reveals its 3D structure. The produced SiO_2 colloidal crystal template paved the way for the next procedure of SERS substrates fabrication.
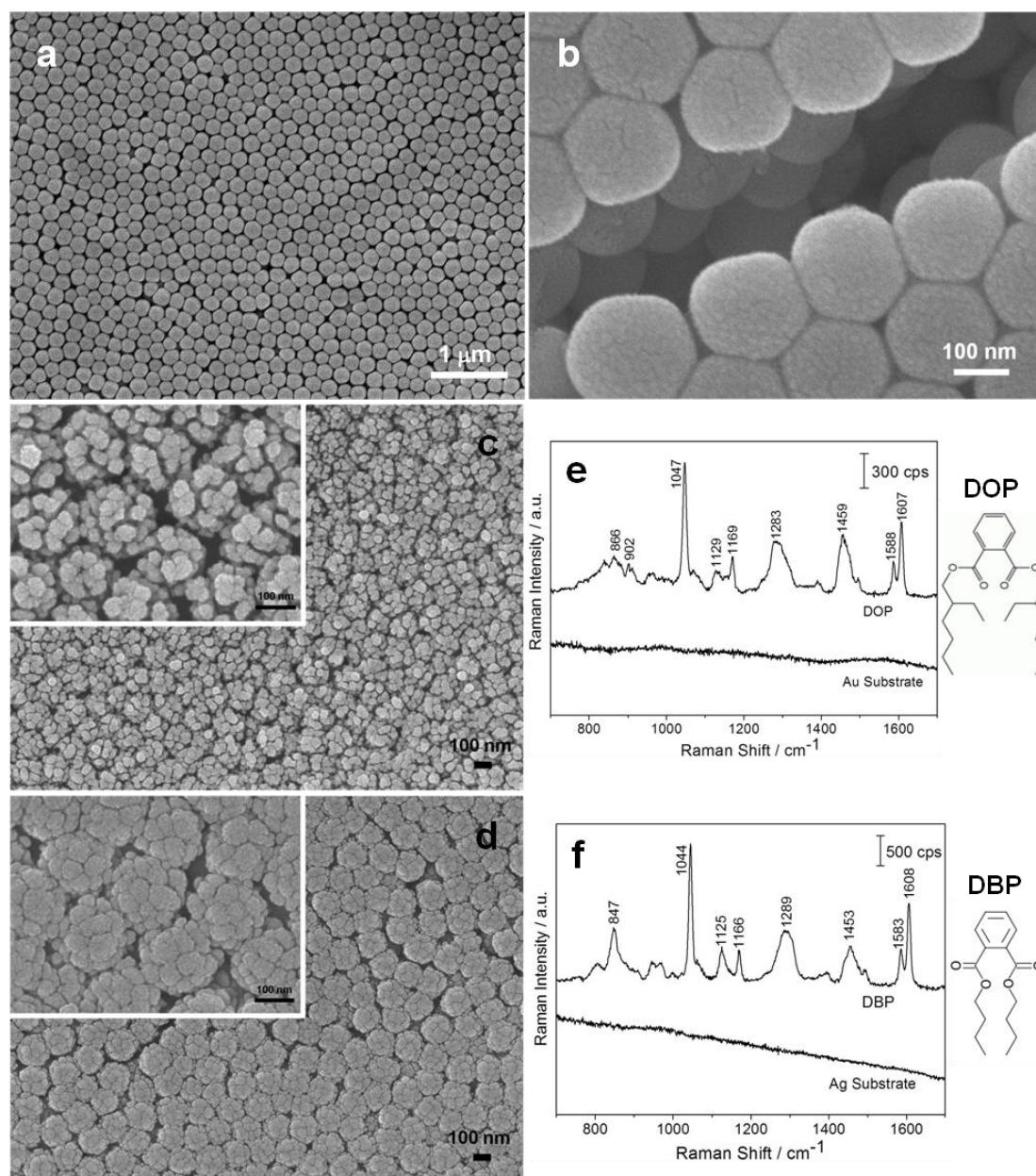
Figure 1 (a,b) FE-SEM images of SiO$_2$ colloidal crystal on a silicon wafer, and (b) reveals a crevice of SiO$_2$ colloidal crystal. FE-SEM images of SERS substrates after deposition of (c) Au and (d) Ag nanoparticles onto the SiO$_2$ colloidal crystal templates, respectively (the deposition time were both 180 s), and the insets show the corresponding high-magnification images. (e) Top: SERS spectrum of 10^{-6} M DOP methanol solution acquired from SiO$_2$ colloidal crystal-assisted Au SERS substrate; bottom: SERS spectrum obtained from the Au SERS substrate without being dripped any EDCs. (f) Top: SERS spectrum of 10^{-6} M DBP methanol solution acquired from SiO$_2$ colloidal crystal-assisted Ag SERS substrate; bottom: SERS spectrum obtained from the Ag SERS substrate without being dripped any EDCs. Excitation wavelength: 785 nm; laser power: 8 mW. The collected time is 15 s exposure time and 5 scans. The structural formulas of DOP, DBP are displayed on the right side of Figure1e, 1f, respectively.
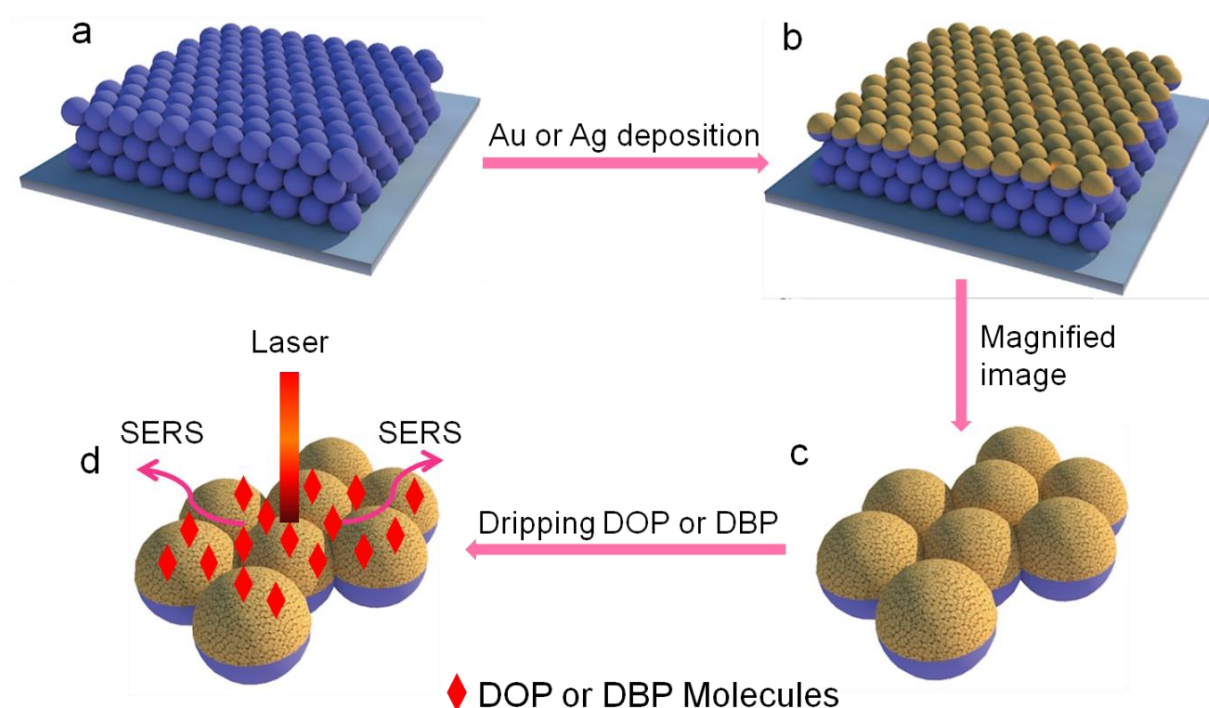
Scheme 1 Schematic diagrams of fabrication of SiO_2 colloidal crystal-assisted Au, Ag SERS substrates and identification of EDCs. (a) SiO_2 colloidal crystal assembled on a silicon wafer; (b) after deposition of Au or Ag nanoparticles on the SiO_2 colloidal crystal; (c) the corresponding high-magnification image; (d) SERS detection of DOP or DBP molecules by the SiO_2 colloidal crystal-assisted Au, Ag SERS substrates.

3.2 Fabrication of SiO_2 colloidal crystal-assisted Au and Ag SERS substrates, and SERS identification of two EDCs.

Noble metal nanoparticles deposition on the substrates is a powerful technique for nanostructure fabrication. Instead of the deposition on the uncovered substrates directly, fabrication based on monolayer colloidal crystals or multilayer colloidal crystals is also an effective approach for producing a wide variety of nanostructures.[77] Different nanostructures with various morphologies can be produced by choosing proper deposition techniques and deposition conditions, and then the morphology-dependent properties and applications can be explored.[77]

Here SiO_2 multilayer colloidal crystal template was used as the substrate, and Au,

Ag nanoparticles were deposited onto the SiO_2 spheres by employing a versatile nanocluster fabrication system (NanoSys 2, Oxford Applied Research Inc.). The QMF was turned on during the deposition process to control the nanoparticle size distribution, and a series of parameters were set to let the nanoparticle size around 10 nm can pass through and reach the SiO_2 colloidal crystal template. The fabrication of SiO_2 colloidal crystal-assisted Au, Ag SERS substrates, and the identification of EDCs are illustrated in Scheme 1.

Firstly, the deposition time was explored (see Supporting Information), and 180 s was set as the optimal deposition time in this work. Figure 1c and Figure 1d are the corresponding FE-SEM images of SERS substrates after deposition of Au and Ag nanoparticles onto the SiO_2 colloidal crystal templates, respectively (the deposition time were both 180 s). The insets in Figure 1c and Figure 1d show the corresponding high-magnification images. Interestingly, unique broccoli-shaped profiles were produced through this versatile nanofabrication system with proper deposition conditions, and large-area patterned broccoli-like Au, Ag SERS arrays were obtained. Compared to the conventional MFON substrates,[71] the highly rough surface feature and the enlarged surface area, together with large amounts of "hot spots" arise from the close interparticle distance on each "flower head", enable this broccoli-shaped SERS array to have a greater Raman amplification.

Next, the broccoli-shaped Au and Ag SERS substrate were applied to detect two EDCs, *i.e.* DOP and DBP, respectively. From Figure 1e, 1f, the SERS spectra of DOP and DBP (10^{-6} M, methanol solutions) were well obtained with a good ratio of signal

to noise, and the sharp, distinguishable vibrational fingerprints they present delivered the inherent structural information of EDC molecules. DOP and DBP are homologous series (their structural formulas displayed on the right side of Figure 1e, 1f), and the acquired SERS spectra display different features. The major differences between these two SERS spectra are in the region of 780~920 cm^{-1} and 1100~1150 cm^{-1}, which are assigned to the C-H out-of-plane bend and C-O stretch, respectively.[78] The fact that the colloidal crystal-assisted Au and Ag SERS substrates in this work have the ability to distinguish homologous series, suggesting the broccoli-shaped SERS array have a high sensitivity and their potentially wide applications in chemical molecules detection. Two flat SERS spectra at the bottom of Figure 1e, 1f were acquired from the broccoli-shaped Au, Ag SERS substrates without being dripped any EDCs. No obvious Raman peaks could be detected indicating the clean surfaces without incorporating any reductants or surfactant chemicals, which is the fundamental principle for reliable SERS detection.

3.3 SERS reproducibility

Reproducibility is an important index to evaluate the performance of SERS substrates. Here, we chose R6G as the probe molecules to explore the reproducibility of SiO$_2$ colloidal crystal-assisted Au and Ag SERS substrates. 10 μL of 10^{-4} M R6G solution was dripped on these two SERS substrates, and SERS spectra from 5 random-selected spots on each SERS substrate were acquired under identical experimental conditions. The SERS spectra of R6G in these five different positions are fairly consistent with each other in terms of Raman peaks as well as Raman

intensity (Figure 2a, 2b). Figure 2c gives an even clearer clarification, from which the relative standard deviations (RSDs) of the peak intensity at 772 cm^{-1} are about 8.7% and 5.7% for Figure 2a, 2b, respectively. The low RSDs indicate the good reproducibility and suggest the fabricated SiO_2 colloidal crystal-assisted Au and Ag SERS substrates in this work are reliable and good candidates for EDCs detection.
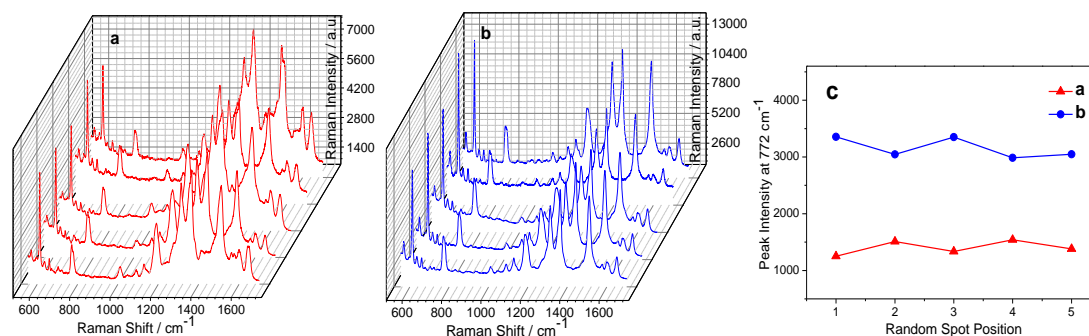

Figure 2 SERS spectra of 10^{-4} M R6G acquired from 5 random-selected places on SiO_2 colloidal crystal-assisted (a) Au and (b) Ag SERS substrates (the deposition time were both 180 s), respectively. Excitation wavelength: 785 nm; laser power: 0.8 mW. The collected time is 15 s exposure time and 5 scans. (c) Plots of the peak intensities of R6G at 772 cm^{-1} obtained from 5 random places on the above two SERS substrates, respectively.

3.4 Electromagnetic simulation and EFs calculation

Numerical simulations were performed using the finite difference time domain (FDTD) method by employing a commercial software package from Lumerical Solutions, Inc., Canada (version 8.7.3), to numerically estimate the electromagnetic field distribution at the surface of Au-coated and Ag-coated plasmonic nanostructures. The Yee cell in our calculation is set to 0.5 nm $\times$ 0.5 nm $\times$ 0.5 nm and perfectly matched layers (PML) were used as a boundary condition. In order to match the experimental system as closely as possible, the models of the structures were developed by extracting from FE-SEM images. Subtle differences were found between Au-coated (Figure 3a) and Ag-coated (Figure 3b) broccoli-shaped SERS

arrays, so typical regions (the area in each red circle in Figure 3a, 3b, respectively) were selected separately for the FDTD simulations. Figure 3c, 3d are the corresponding simulation models extracted from the typical regions in Figure 3a, 3b. Both Au and Ag nanoparticles are treated in spherical shapes and the diameter is 10 nm as the QMF was set at 10.0 nm size selection. The particles in a uniform dielectric medium (n = 1) were illuminated from the top with a linearly polarized plane wave of 785 nm wavelength. The dielectric constant of Au and Ag are from Johnson and Christy.[79] Figure 3e, 3f show the corresponding simulation results of Au-coated and Ag-coated SERS array nanostructures. The electric field magnitude is normalized by dividing the maximum absolute value. The simulation results show that the broccoli-shaped SERS array structures generate localized plasmons and substantial electromagnetic field enhancements are localized in the narrow gaps of the neighboring nanoparticles (The nanoparticles constituted the "flower head" of the broccoli-like SERS array). These interparticle gaps are the "hot spots" which contribute largely to the SERS enhancement.

Next, the enhancement capability of the broccoli-shaped Au, Ag SERS substrates were evaluated by employing R6G as the probe molecules, and the EF of the broccoli-like Au substrate can be calculated as 1.12×10^7, and the EF of the broccoli-like Ag substrate can be calculated as 1.45×10^7 (see Supporting Information for details). Compared to our previous work,[34,72] which depositing Ag or Au nanoparticles on the silicon wafer directly (the EF was 10^5 for Ag substrate and 10^6 for Au substrate in the previous work), the EF of the colloidal crystal-assisted Ag, Au

SERS arrays in this work are testified to improve by 10^2 times and 10 times, respectively, which demonstrates superiority of the broccoli-shaped nanostructure morphology.
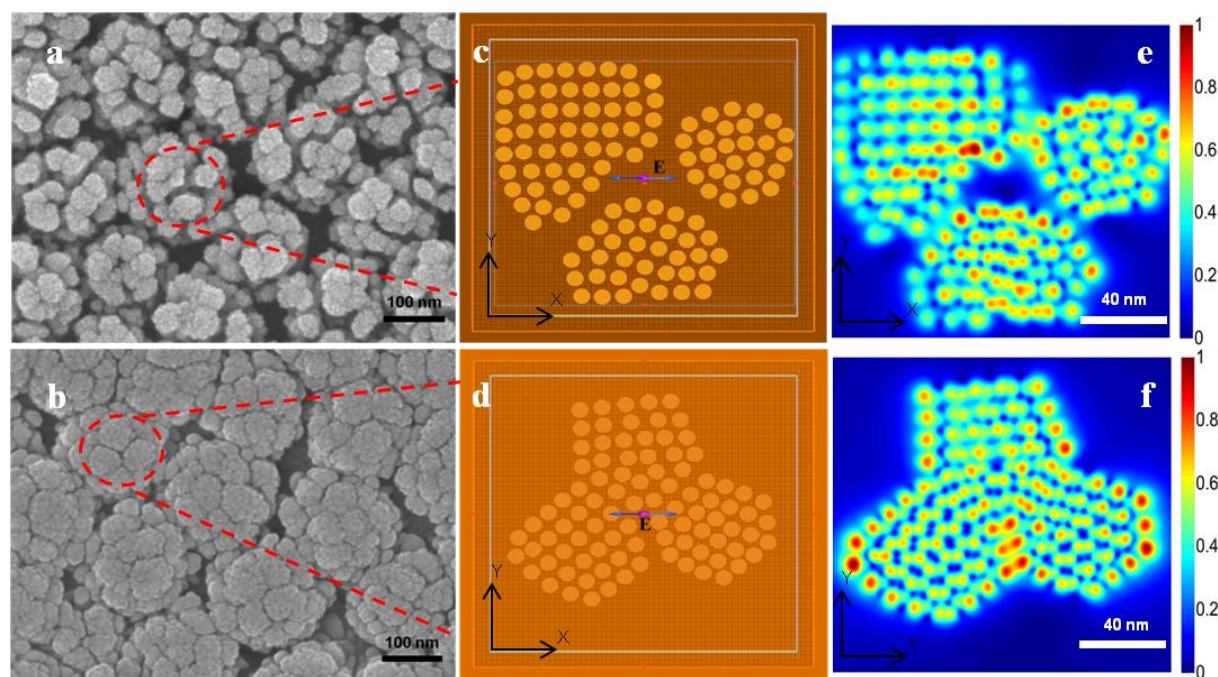

Figure 3 FE-SEM images of (a) Au-coated and (b) Ag-coated broccoli-shaped SERS arrays (the deposition time were both 180 s). The regions in the red circles are the selected areas used for FDTD simulations. Simulation models for (c) Au-coated and (d) Ag-coated SERS arrays. The simulation results of (e) Au-coated and (f) Ag-coated broccoli-shaped SERS arrays.

3.5 Long-term stability of SERS substrates

Besides Raman enhancement and reproducibility, stability is another important index for SERS substrate as an ideal SERS sensor system needs long time, efficient running, which requires long-term stability without being degraded, contaminated, or loss of enhancement. Here SiO_2 colloidal crystal-assisted Au, Ag SERS substrates were detected after they were saved in commercial aluminum foil for 90 days, and R6G was used as the probe molecules (Figure 4). Each SERS spectrum in Figure 4a, 4b is an average result of five random detections focused on different positions.

Compared to the colloid solution system, our SERS substrates display quite stable

property as they will not sediment out of solution. After 90 days, the SERS

enhancement of SiO_2 colloidal crystal-assisted Au substrate was reduced by 31.6%,

and SiO_2 colloidal crystal-assisted Ag substrate was reduced by 51.2% (average

results of the vibration mode at 772 cm^{-1}, 1188 cm^{-1}, and 1508 cm^{-1}) relative to the

SERS spectra in Figure S2b, S2c (Supporting Information), respectively, which were

obtained from the freshly prepared SERS substrates. The long-term stability data of

the broccoli-shaped Au, Ag SERS substrates in this work are comparable to that of

Halas's work[62] and Kim's work[80]. Then we can conclude that in this work the

colloidal crystal-assisted Ag SERS array has a slight higher EF than Au SERS array,

while the latter has a better long-term stability than Ag SERS array, which may result

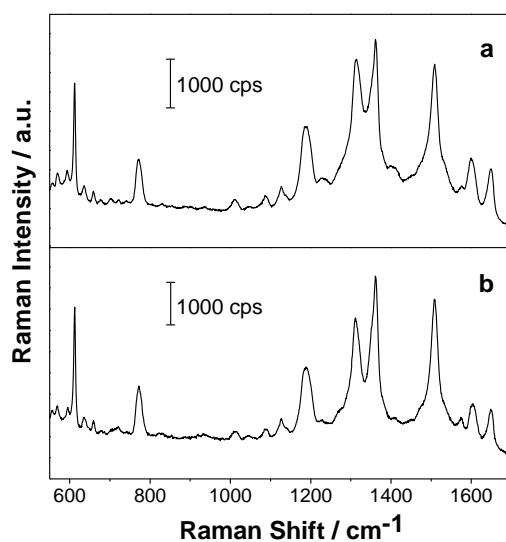from Ag nanoparticles can get oxidized easily under ambient conditions.

Figure 4 SERS spectrum of 10^{-4} M R6G solution acquired from SiO_2 colloidal crystal-assisted (a) Au and (b) Ag SERS substrates after they were kept in commercial aluminum foil under ambient conditions for 90 days. Laser power: 0.8 mW.

3.6 Relationship between SERS intensity and two EDCs concentration

A series of SERS spectra of DOP (Figure 5a) and DBP (Figure 5b) at different

concentrations (10^{-10} to 10^{-3} M, methanol solutions) were detected to demonstrate the sensitivity of the broccoli-shaped SERS substrates. From Figure 5a, 5b, the SERS spectral intensity decreases as the concentration decreases. The detection limits of 0.24×10^{-9} M and 0.22×10^{-9} M were obtained for the broccoli-shaped Au, Ag SERS arrays for detecting DOP, DBP, respectively (according to the signal/noise ratio of three). The correlations between SERS intensity and DOP, DBP concentration were listed in Figure 5c, 5d, respectively. The SERS peak intensity of DOP at 1047 cm^{-1} and DBP at 1044 cm^{-1} was set as y-axis, and DOP, DBP concentration (logarithmic) was set as x-axis.

Two linear relationships exist in the concentration range of 10^{-10} ~ 10^{-3} M for both DOP and DBP. For DOP, when in the concentration range of 10^{-10} ~ 10^{-6} M, the linear regression equation is $y = 327.2 \log(x) + 3229.8$, and the correlation coefficient is 0.991 (n = 5); When in the concentration range of 10^{-6} ~ 10^{-3} M, the linear regression equation is $y = 1506.9 \log(x) + 10238.3$, and the correlation coefficient is 0.996 (n = 4). For DBP, when in the concentration range of 10^{-10} ~ 10^{-5} M, the linear regression equation is $y = 722.1 \log(x) + 7007.1$, and the correlation coefficient is 0.990 (n = 6); When in the concentration range of 10^{-5} ~ 10^{-3} M, the linear regression equation is $y = 2900 \log(x) + 18160$, and the correlation coefficient is 0.999 (n = 3).

According to the two different linear relationships in the whole concentration range, we conjecture that there may exist submonolayer-monolayer adsorption (in the low-concentration range) and multilayer adsorption (in the high-concentration range), following two different types of adsorption isotherms respectively[81,82]. In the

low-concentration region, since all the analyte molecules contact with the SERS substrate surface directly, and SERS has proximity effect, SERS intensity will increase sharply as the analyte concentration increases. While in the high-concentration region, because of the multilayer adsorption, SERS intensity increase will become slower. We should note that, in Figure 5c, 5d, the x-axis has been taken the logarithm, so the slopes in the low-concentration region are smaller than that in the high-concentration region. In Cheng's paper[82], this piecewise linear phenomenon has also been reported, and they also mentioned the fact that the slope in the high-concentration linear range was smaller than that for the low-concentration linear range (x-axis was not taken the logarithm) reflected multilayer adsorption responsible for the weak enhancement[82]. In Figure 5c, 5d, the inflection point of the piecewise linearity of DOP comes at a lower concentration (10^{-6} M) in comparison with DBP's (10^{-5} M), and this may result from DOP has a larger molecular 3D structure than DBP, thus monolayer adsorption saturation comes at a lower concentration than that for DBP.
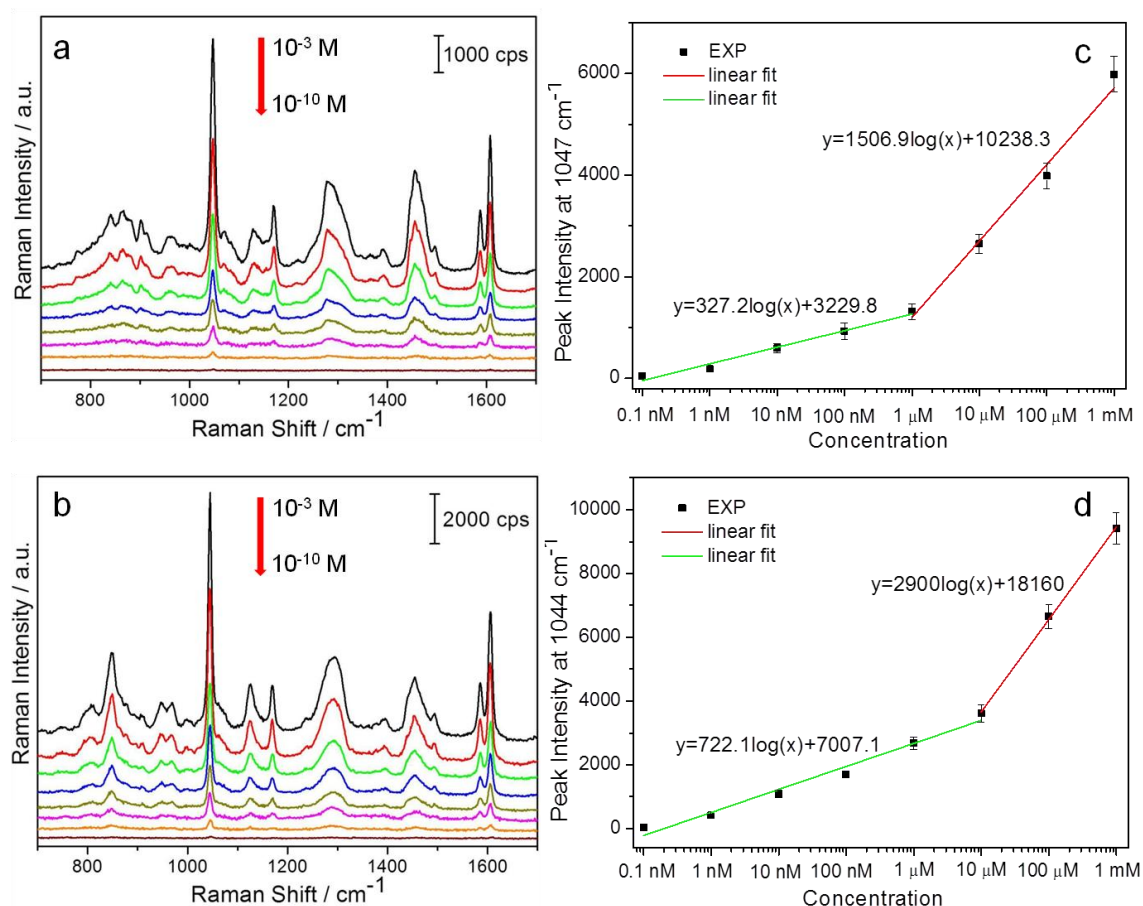
Figure 5 Concentration-dependent SERS spectra of (a) DOP ($10^{-10} \sim 10^{-3}$ M, methanol solutions), which were obtained from the broccoli-shaped Au SERS substrate, and (b) DBP ($10^{-10} \sim 10^{-3}$ M, methanol solutions), which were obtained from the broccoli-shaped Ag SERS substrate. Excitation wavelength: 785 nm; laser power: 8 mW. Piecewise linear plots of (c) DOP SERS intensity at 1047 cm^{-1} *vs.* DOP concentration in (a), and (d) DBP SERS intensity at 1044 cm^{-1} *vs.* DBP concentration in (b).

4. Conclusions

Au and Ag nanoparticles were deposited onto SiO_2 multilayer colloidal crystal templates, respectively by a versatile nanocluster fabrication system and broccoli-shaped Au, Ag SERS substrates were produced. This SERS array has a long-range, controllable periodic structure, and also with a clean surface without incorporating any reductants or surfactant chemicals. The broccoli-shaped SERS morphology creates an increased roughness and a larger surface area, resulting in a

greater Raman amplification than the conventional MFON. SERS performances by these two SERS arrays reveal that this long-range broccoli-like morphology is a promising SERS platform as it is highly sensitive, reproducible, and has long-term stability. The EFs of the two broccoli-like Au, Ag SERS arrays are both high up to 10^7. Compared to our previous work which depositing noble metal nanoparticles onto the flat substrates directly, the EF of the colloidal crystal-assisted SERS array is improved by one to two orders of magnitude. The FDTD simulation results show that substantial electromagnetic field enhancement exists in the gaps between nanoparticles on the "flower head". Finally, two EDCs (*i.e.* DOP and DBP, methanol solutions) at different concentrations were successfully identified by the broccoli-like Au, Ag SERS substrates with the detection limits of 0.24×10^{-9} M and 0.22×10^{-9} M, respectively. It is hopeful that this colloidal crystals-assisted nanostructure arrays with the unique broccoli-shaped profile will become a promising candidate in SERS sensing.

Supporting Information Available: FE-SEM images of SiO_2 colloidal crystal-assisted Ag SERS substrates at different deposition time (90 s, 180 s, and 300 s). EFs calculation of the broccoli-shaped Au, Ag SERS substrates.

Acknowledgements

References

[1] http://www.niehs.nih.gov/health/topics/agents/endocrine/

[2] http://en.wikipedia.org/wiki/Endocrine_disruptor

[3] Harrison, R. M.; Hester, R. E. *Endocrine Disrupting Chemicals*; Royal Society of Chemistry: Cambridge, UK, 1999.

[4] Yang, J.; Hauser, R.; Goldman, R. H. *Food Chem. Toxicol.* 2013, 58, 362-368.

[5] Wu, M. T.; Wu, C. F.; Wu, J. R.; Chen, B. H.; Chen, E. K.; Chao, M. C.; Liu, C. K.; Ho, C. K. *Environ. Int.* 2012, 44, 75-79.

[6] Preedy, V. R. *Handbook of Growth and Growth Monitoring in Health and Disease, Volume 1*; Springer, 2012 edition.

[7] Heudorf, U.; Mersch-Sundermann, V.; Angerer, J. *Int. J. Hyg. Envir. Heal.* 2007, 210, 623-634.

[8] Koch, H. M.; Haller, A.; Weiss, T.; Kafferlein, H. U.; Stork, J.; Bruning, T. *Toxicol. Lett.* 2012, 213, 100-106.

[9] Fang, C.; Bandaru, N. M.; Ellis, A. V.; Voelcker, N. H. *Biosens. Bioelectron.* 2013, 42, 632-639.

[10] Yen, T. H.; Lin-Tan, D. T.; Lin, J. L. *J. Formos. Med. Assoc.* 2011, 110, 671-684.

[11] Tranfo, G.; Caporossi, L.; Paci, E.; Aragona, C.; Romanzi, D.; De Carolis, C.; De

Rosa, M.; Capanna, S.; Papaleo, B.; Pera, A. *Toxicol. Lett.* 2012, 213, 15-20.

[12] Sanchez-Avila, J.; Tauler, R.; Lacorte, S. *Environ. Int.* 2012, 46, 50-62.

[13] Fierens, T.; Van Holderbeke, M.; Willems, H.; De Henauw, S.; Sioen, I. *Food Chem Toxicol.* 2012, 50, 2945-2953.

[14] Cheung, W.; Shadi, I. T.; Xu, Y.; Goodacre, R. *J. Phys. Chem. C* 2010, 114, 7285-7290.

[15] Nie, S. M.; Emory, S. R. *Science* 1997, 275, 1102–1106.

[16] Kneipp, K.; Wang, Y.; Kneipp, H.; Perelman, L. T.; Itzkan, I.; Dasari, R.; Feld, M. S. *Phys. Rev. Lett.* 1997, 78, 1667–1670.

[17] Zhang, R.; Zhang, Y.; Dong, Z. C.; Jiang, S.; Zhang, C.; Chen, L. G.; Zhang, L.; Liao, Y.; Aizpurua, J.; Luo, Y.; Yang, J. L.; Hou, J. G. *Nature* 2013, 498, 82-86.

[18] Kleinman, S. L.; Ringe, E.; Valley, N.; Wustholz, K. L.; Phillips, E.; Scheidt, K. A.; Schatz, G. C.; Van Duyne, R. P. *J. Am. Chem. Soc.* 2011, 133, 4115-4122.

[19] Michaels, A. M.; Nirmal, M.; Brus, L. E. *J. Am. Chem. Soc.* 1999, 121, 9932-9939.

[20] Moyer, P. J.; Schmidt, J.; Eng, L. M.; Meixner, A. J. *J. Am. Chem. Soc.* 2000, 122, 5409-5410.

[21] Qian, X. M.; Nie, S. M. *Chem. Soc. Rev.* 2008, 37, 912-920.

[22] Lim, D. K.; Jeon, K. S.; Kim, H. M.; Nam, J. M.; Suh, Y. D. *Nat. Mater.* 2010, 9, 60-67.

[23] Camden, J. P.; Dieringer, J. A.; Zhao, J.; Van Duyne, R. P. *Accounts Chem. Res.* 2008, 41, 1653-1661.

[24] Qian, X. M.; Peng, X. H.; Ansari, D. O.; Yin-Goen, Q.; Chen, G. Z.; Shin, D. M.; Yang, L.; Young, A. N.; Wang, M. D.; Nie, S. M. *Nat. Biotechnol.* 2008, 26, 83-90.

[25] Driskell, J. D.; Seto, A. G.; Jones, L. P.; Jokela, S.; Dluhy, R. A.; Zhao, Y. P.; Tripp, R. A. *Biosens. Bioelectron.* 2008, 24, 917-922.

[26] Pozzi, E. A.; Sonntag, M. D.; Jiang, N.; Klingsporn, J. M.; Hersam, M.; Van Duyne, R. P. *ACS Nano* 2013, 7, 885-888.

[27] Wang, G. F.; Lipert, R. J.; Jain, M.; Kaur, S.; Chakraboty, S.; Torres, M. P.; Batra, S. K.; Brand, R. E.; Porter, M. D. *Anal. Chem.* 2011, 83, 2554-2561.

[28] Lee, M.; Lee, S.; Lee, J. H.; Lim, H. W.; Seong, G. H.; Lee, E. K.; Chang, S. I.; Oh, C. H.; Choo, J. *Biosens. Bioelectron.* 2011, 26, 2135-2141.

[29] Sha, M. Y.; Xu, H.; Penn, S. G.; Cromer, R. *Nanomedicine* 2007, 2, 725-734.

[30] Shanmukh, S.; Jones, L.; Driskell, J.; Zhao, Y. P.; Dluhy, R.; Tripp, R. A. *Nano Lett.* 2006, 6, 2630-2636.

[31] Negri, P.; Kage, A.; Nitsche, A.; Naumann, D.; Dluhy, R. A. *Chem. Commun.* 2011, 47, 8635-8637.

[32] Dougan, J. A.; MacRae, D.; Graham, D.; Faulds, K. *Chem. Commun.* 2011, 47, 4649-4651.

[33] Combs, Z. A.; Chang, S.; Clark, T.; Singamaneni, S.; Anderson, K. D.; Tsukruk, V. V. *Langmuir* 2011, 27, 3198-3205.

[34] Chen, J.; Qin, G. W.; Wang, J. S.; Yu, J. Y.; Shen, B.; Li, S.; Ren, Y. P.; Zuo, L.; Shen, W.; Das, B. *Biosens. Bioelectron.* 2013, 44, 191-197.

[35] Chen, J.; Shen, B.; Qin, G. W.; Hu, X. W.; Qian, L. H.; Wang, Z. W.; Li, S.; Ren,

Y. P.; Zuo, L. *J. Phys. Chem. C* 2012, 116, 3320-3328.

[36] Smith-Palmer, T.; Douglas, C.; Fredericks, P. *Vib. Spectrosc.* 2010, 53, 103-106.

[37] Zhang, X. Y.; Young, M. A.; Lyandres, O.; Van Duyne, R. P. *J. Am. Chem. Soc.* 2005, 127, 4484-4489.

[38] Han, X. X.; Zhao, B.; Ozaki, Y. *Anal. Bioanal. Chem.* 2009, 394, 1719-1727.

[39] Barhoumi, A.; Halas, N. J. *J. Am. Chem. Soc.* 2010, 132, 12792-12793.

[40] Hong, G. S. Li, C.; Qi, L. M. *Adv. Funct. Mater.* 2010, 20, 3774-3783.

[41] Stokes, D. L.; Pal, A.; Narayanan, V. A.; Vo-Dinh, T. *Anal. Chim. Acta* 1999, 15, 265-274.

[42] Stuart, D. A.; Biggs, K. B.; Van Duyne, R. P. *Analyst* 2005, 131, 568-572.

[43] Piorek, B. D.; Lee, S. J.; Santiago, J. G.; Moskovits, M.; Banerjee, S.; Meinhart, C. D. *Proc. Natl. Acad. Sci. U.S.A.* 2007, 104, 18898-18901.

[44] Lin, M.; He, L.; Awika, J.; Yang, L.; Ledoux, D. R.; Li, H.; Mustapha, A. *J. Food Sci.* 2008, 73, 129-134.

[45] Golightly, R. S.; Doering, W. E.; Natan, M. J. *ACS Nano* 2009, 3, 2859-2869.

[46] Halvorson, R. A.; Vikesland, P. J. *Environ. Sci. Technol.* 2010, 44, 7749-7755.

[47] Kong, K. V.; Lam, Z. Y.; Lau, W. K. O.; Leong, W. K.; Oivo, M. *J. Am. Chem. Soc.* 2013, 135, 18028-18031.

[48] An, Q.; Zhang, P.; Li, J. M.; Ma, W. F.; Guo, J.; Hu, J.; Wang, C. C. *Nanoscale* 2012, 4, 5210-5216.

[49] Li, X. Z.; Zhang, S.; Yu, Z.; Yang, T. Y. *Appl. Spectrosc.* 2014, 68, 483-487.

[50] Luo, S. C.; Sivashanmugan, K.; Liao, J. D.; Yao, C. K.; Peng, H. C. *Biosens.*

Bioelectron. 2014, 61, 232-240.

[51] Cialla, D.; Marz, A.; Bohme, R.; Theil, F.; Weber, K.; Schmitt, M.; Popp, J. *Anal. Bioanal. Chem.* 2012, 403, 27-54.

[52] Wang, Y. Q.; Yan, B.; Chen, L. X. *Chem. Rev.* 2013, 113, 1391-1428.

[53] Kleinman, S. L.; Frontiera, R. R.; Henry, A. I.; Dieringer, J. A.; Van Duyne, R. P. *Phys. Chem. Chem. Phys.* 2013, 15, 21-36.

[54] Jackson, J. B.; Halas, N. J. *Proc. Natl. Acad. Sci. U.S.A.* 2004, 101, 17930-17935.

[55] Prucek, R.; Panacek, A.; Soukupova, J.; Novotny, R.; Kvitek, L. *J. Mater. Chem.* 2011, 21, 6416-6420.

[56] Christou, K.; Knorr, I.; Ihlemann, J.; Wackerbarth, H.; Beushausen, V. *Langmuir* 2010, 26, 18564-18569.

[57] Schutz, M.; Steinigeweg, D.; Salehi, M.; Kompe, K.; Schlucker, S. *Chem. Commun.* 2011, 47, 4216-4218.

[58] Xie, J. P.; Zhang, Q. B.; Lee, J. Y.; Wang, D. I. C. *ACS Nano* 2008, 2, 2473-2480.

[59] Fu, J. J.; Ye, W. C.; Wang, C. M. *Mater. Chem. Phys.* 2013, 141, 107-113.

[60] Fang, J. X.; Du, S. Y.; Lebedkin, S.; Li, Z. Y.; Kruk, R.; Kappes, M.; Hahn, H. *Nano Lett.* 2010, 10, 5006-5013.

[61] Yang, M.; Alvarez-Puebla, R.; Kim, H. S.; Aldeanueva-Potel, P.; Liz-Marzan, L. M.; Kotov, N. A. *Nano Lett.* 2010, 10, 4013-4019.

[62] Wang, H. ; Levin, C. S. ; Halas, N. J. *J. Am. Chem. Soc.* 2005, 127, 14992-14993.

[63] Lim, D. K.; Jeon, K. S.; Hwang, J. H.; Kim, H.; Kwon, S.; Suh, Y. D.; Nam, J. M. *Nat. Nanotechnol.* 2011, 6, 452-460.

[64] Alexander, K. D.; Hampton, M. J.; Zhang, S. P.; Dhawan, A.; Xu, H. X.; Lopez, R. *J. Raman Spectrosc.* 2009, 40, 2171-2175.

[65] Yu, Q. M.; Guan, P.; Qin, D.; Golden, G.; Wallace, P. M. *Nano Lett.* 2008, 8, 1923-1928.

[66] Theiss, J.; Pavaskar, P.; Echternach, P. M.; Muller, R. E. Cronin, S. B. *Nano Lett.* 2010, 10, 2749-2754.

[67] Luo, Z. X.; Peng, A. D.; Fu, H. B.; Ma, Y.; Yao, J. N.; Loo, B. H. *J. Mater. Chem.* 2008, 18, 133-138.

[68] Garrett, N. L.; Vukusic, P.; Ogrin, F.; Sirotkin, E.; Winlove, C. P.; Moger, J. *J. Biophoton.* 2009, 2, 157-166.

[69] Li, J. M.; Ma, W. F.; Wei, C.; Guo, J.; Hu, J.; Wang, C. C. *J. Mater. Chem.* 2011, 21, 5992-5998.

[70] Rao, Y. Y.; Chen, Q. F.; Dong, J.; Qian, W. P. *Analyst* 2011, 136, 769-774.

[71] Dick, L. A.; McFarland, A. D.; Haynes, C. L.; Van Duyne, R. P. *J. Phys. Chem. B* 2002, 106, 853-860.

[72] Chen, J.; Shen, W.; Biswajit, D.; Li, Y. Y.; Qin, G. W. *RSC Adv.* 2014, 4, 22660-22668.

[73] Lu, L.; Eychmuller, A. *Accounts Chem. Res.* 2008, 41, 244-253.

[74] Culha, M.; Cullum, B.; Lavrik, N.; Klutse, C. K. *J. Nanotechnol.* 2012, 971380.

[75] Zhang, T. R.; Zhang, Q.; Ge, J. P.; Goebl, J.; Sun, M. W.; Yan, Y. S.; Liu, Y. S.; Chang, C. L.; Guo, J. H.; Yin, Y. D. *J. Phys. Chem. C* 2009, 113, 3168-3175.

[76] Banerjee, A.; Das, B. *Rev. Sci. Instrum.* 2008, 79, 033910.

[77] Ye, X. Z.; Qi, L. M. *Nano Today* 2011, 6, 608-631.

[78] Rubinson, K. A.; Rubinson, J. F. *Contemporary Instrumental Analysis*; Prentice Hall, United States, 1999.

[79] Johnson, P. B.; Christy, R. W. *Phys, Rev. B* 1972, 6, 4370-4379.

[80] Choi, S.; Ahn, M.; Kim, J. *Anal. Chim. Acta.* 2013, 779, 1-7.

[81] Brunauer, S.; Deming, L. S.; Deming, W. E.; Teller, E. *J. Am. Chem. Soc.* 1940, 62, 1723-1732.

[82] Cheng, H. W.; Huan, S. Y.; Wu, H. L.; Shen, G. L.; Yu, R. Q. *Anal. Chem.* 2009, 81, 9902-9912.
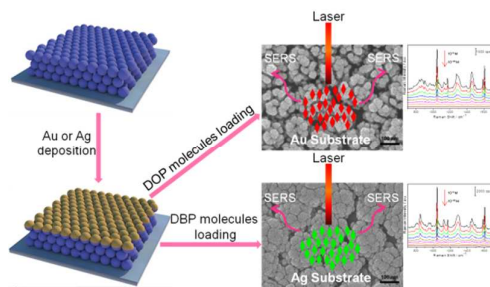
3D periodic broccoli-like Au, Ag SERS arrays with reliability, reproducibility, long-term stability, and high-sensitivity have been fabricated, and are used for detecting phthalates.